A Study on Variance of Maximum Responses of Elasto-plastic Structure Subjected to Artificial Earthquake Ground Motions

I. Ichihashi & A. Sone & A. Masuda & T. Noma
Dept. of Mechanical and System Engineering, Kyoto InstituteTechnology,Kyoto, Japan

SUMMARY:
A number of artificial earthquake ground motions compatible with time-frequency characteristics of recorded actual earthquake ground motions as well as the given target response spectrum are generated using wavelet transform. The coefficient of variation (C. O. V.) of maximum displacement, maximum velocity and maximum acceleration in elasto-plastic SDOF systems excited by these artificial ground motions are numerically evaluated. The C. O. V. of maximum responses based on different time-frequency characteristics of artificial ground motions, different input intensity and different natural periods of SDOF systems are compared. The trajectory of mass around maximum displacement and the variances of displacement with maximum displacements are shown. It is recognized that the C. O. V. become large as input intensity is large and as natural period is small. It is also recognized that the variances of displacements jump and reach the maximum value at the moment occurred plastic drift in displacement. And the fluctuation of variances of displacement fairly corresponds with that of maximum values of displacement.

Keywords: Seismic motion, earthquake resistant, nonlinear vibration, wavelet transform, variation of response

1. INTRODUCTION

For the design basis earthquake ground motions of structure are usually defined to be compatible with the design response spectrum. It has been known that the maximum values of elasto-plastic responses of structure subjected to a group of artificial earthquake ground motions generated to be compatible with the given design response spectrum change in no small way (Kitahara and Itoh, 2001). The input energy to the structure from an earthquake ground motion shows the non-stationary time history due to its time-frequency characteristics and nonlinearity of structures, and it is known that the damage rate of the structure depends on this non-stationary characteristics (Kuwamura et al., 1997).

As for the synthesis of the artificial earthquake ground motion considering the non-stationary characteristics of ground motion, the method using Fourier phase characteristics (Kimura, 1986) and the method using wavelet transform (Maeda et. al., 2002) are proposed. Masuda et al. proposed the method generating the artificial earthquake ground motion compatible with the given response spectrum and having non-stationary time-frequency characteristics by using wavelet transform of velocity response function (Masuda and Sone, 2002a and Masuda and Sone, 2002b). Kubo et al. evaluated the mean value of ductility factor in inelastic responses of SDOF structure subjected to strong earthquake motions with non-stationary frequency contents for hysteresis characteristics, input intensity and so on (Kubo et al., 1989). In the previous papers, a number of artificial ground motions were generated by Masuda's method, and elasto-plastic response analyses were carried out to examine the variance of the structural response in the elasto-plastic region (Ichihashi et al. , 2010a and Ichihashi et al. , 2010b)

A number of artificial earthquake ground motions compatible with time-frequency characteristics of recorded actual earthquake ground motions as well as the given target response spectrum are generated using wavelet transform. The coefficient of variation (C. O. V.) of maximum displacement, maximum

velocity and maximum acceleration in elasto-plastic SDOF systems excited by these artificial ground motions are numerically evaluated. The C. O. V. based on different time-frequency characteristics of artificial ground motions, different input intensity and different natural periods of SDOF systems are compared. The trajectory of mass around maximum displacement and the variances of displacement with maximum displacements are shown. It is recognized that the C. O. V. become large as input intensity is large and as natural period is small. It is also recognized that the variances of displacements jump and reach the maximum value at the moment occurred plastic drift in displacement. And the fluctuation of variances of displacement fairly corresponds with the fluctuation of maximum values of displacement.

2. GENERATION OF ARTIFICIAL EARTHQUAKE GROUND ACCELERATION

We generate the artificial earthquake ground motion by wavelet transform using impulse velocity response function as analyzing wavelet. If the function which reversed the time axis for the impulse velocity response function of a SDOF system of natural period T=1 is defined as the analyzing wavelet $\psi(t)$, then the relative velocity response spectrum $S_V(T, \zeta)$ is given by the wavelet transform of artificial earthquake ground acceleration $\ddot{x}_g$ as Eqn.(1).

$$S_V(T,\zeta) = \max_t \left| \int_{-\infty}^{\infty} \psi\left(\frac{t-\tau}{T}\right) \ddot{x}_g \, d\tau \right| \tag{1}$$

where

$$\begin{cases} \psi(t) = 0 & (t > 0) \\ \psi(t) = -e^{2\pi\zeta t}\left(\cos 2\pi\sqrt{1-\zeta^2}\,t + \dfrac{\zeta}{\sqrt{1-\zeta^2}} \sin 2\pi\sqrt{1-\zeta^2}\right) & (t \le 0) \end{cases} \tag{2}$$

Also, ζ is the damping ratio of a SDOF system. Therefore, using this relation, we can compose the ground acceleration compatible to the given design response spectrum and the given time-frequency characteristic through inverse wavelet transform.

In this study, the Osaki's spectrum (Osaki, 1994) for the magnitude of 7 and the epicenter distance of 20 km of earthquake, shown in Fig.1, is adopted as the design spectrum. Five time-frequency functions derived actual recorded ground motions which recently caused extensive damage against structures or maximum ground acceleration more than 1 m/s^2 in Japan are adopted as the target time-frequency characteristics to generate the artificial ground motions. The list of selected actual ground motions is shown in Table 1.

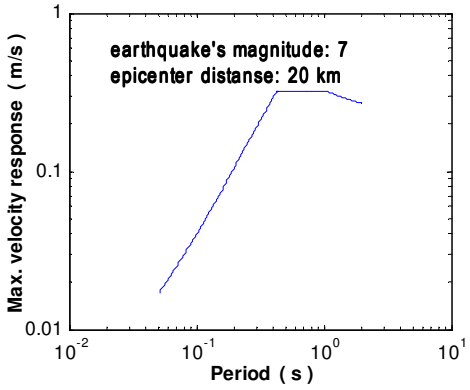

Figure 1. Osaki's spectrum

Table 1. List of earthquake ground motions

No.	Origin time	Location of observation	Maximum acceleration
1	2011/03/11/14:46	Tsukidate	27.0 m/s2
2	2011/03/11/14:46	Hitachi	16.0
3	2007/07/16/10:13	Kashiwazaki	5.14
4	2004/11/29//03:32	Nosapu	5.50
5	2004/10/23/17:56	Ojiya	13.1

30 artificial earthquake ground accelerations are generated for each of five time-frequency characteristics. The examples of artificial earthquake ground accelerations in the cases of No.1,

No.3 and No.4 are shown in Fig.2, and the comparison among the target velocity response spectrum and their velocity response spectra is shown in Fig.3, respectively. Since the mean value of the coefficient of variation (C. O. V.) of linear velocity response spectrum due to each artificial ground acceleration from the period in the linear range of structure of 0.05 to 2.0s is almost from 0.0421 to 0.055, both velocity response spectra agree well. Also, the examples of time-frequency functions obtained by real earthquake motions are shown in Figs.4-8.

3. RESPONSE OF ELASTO-PLASTIC STRUCTURE EXCITED BY ARTIFICIAL EARTHQUAKE GROUND MOTION

The hysteretic restoring force of structure is assumed to be as bi-linear restoring force model in Fig. 9. And the ratio of the post-yield stiffness k_p to the initial stiffness before yield k_e is assumed to be 1/100. In this paper, we consider the response of SDOF structure composed of a mass m, stiffness with bi-linear hysteresis restoring force and viscous damping c as shown in Fig. 10. The equation of motion of this structure, when it is subjected to a base acceleration $\ddot{x}_g$, is expressed as Eqn.(3).

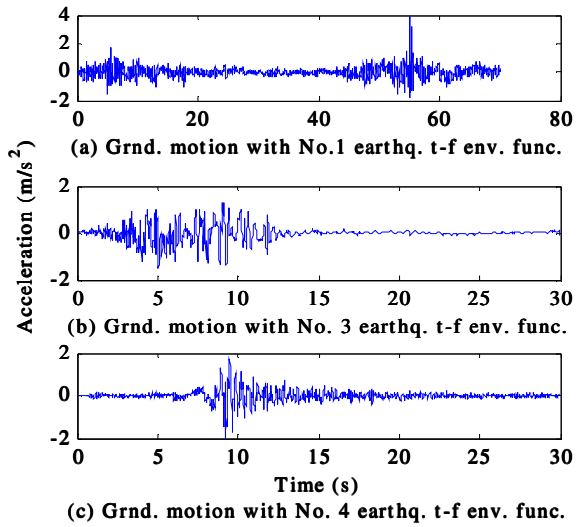

Figure2. Examples of generated ground motions

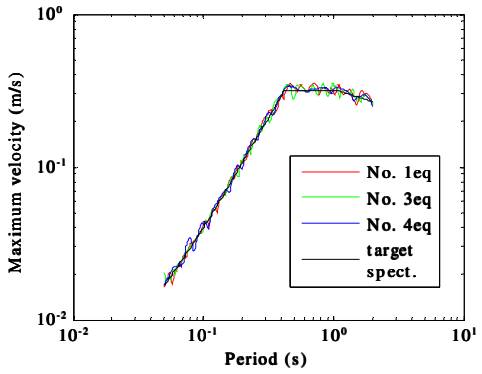

Figure3. Spectral velocity response

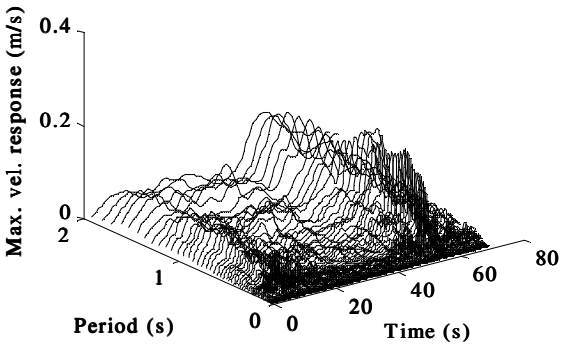

Figure4. Time-frequency characteristic of No.1 earthquake

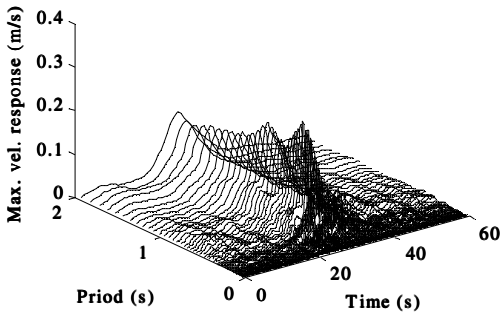

Figure 5. Time-frequency characteristic of No.2 earthquake

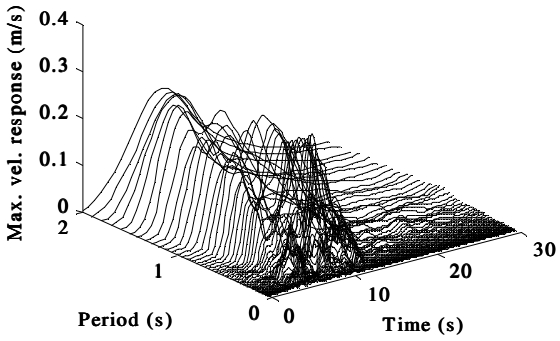

Figure6. Time-frequency characteristic of No.3 earthquake

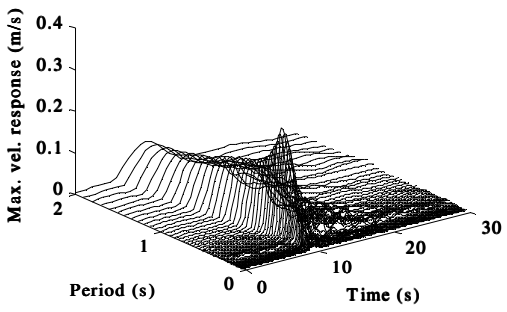

Figure7. Time-frequency characteristic of No.4 earthquake

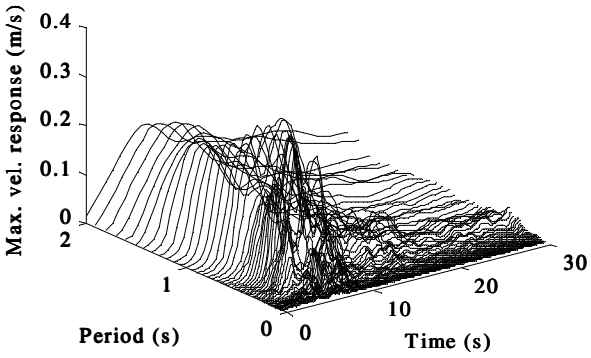

Figure8. Time-frequency characteristic of No.5 earthquake

$$m\ddot{x} + c\dot{x} + F(x) = -m\ddot{x}_g \tag{3}$$

In this paper, the Eqn. (3) is solved numerically by linear acceleration method for each artificial earthquake motion mentioned above. The natural period $T_0 = 2\pi\sqrt{m/k_e}$ in linear range of structure and the damping ratio $\zeta = c/2\sqrt{mk_e}$ of the viscous damping are taken as T_0 = 0.05 s ~ 2.0 s and ζ= 0.02 respectively. F_y is the yield force and the maximum amplitude of the artificial earthquake acceleration $\ddot{x}_g$ is taken as $m\ddot{x}_g / F_y$ =1.0, 1.2, 1.5, 2.0 (relative input intensity: α) so that the maximum displacement will moderately exceed the yield displacement .

The mean values of C.O.V.s of maximum relative displacement, maximum relative velocity and maximum relative acceleration for T_0=0.2, 0.5 and 1.0 s are shown in Tables 2-4. From Table 2, it is clear that C.O.V. of maximum relative displacement almost increases as the relative input intensity α increases. However, this tendency is not shown in the cases of C.O.V.s of maximum relative velocity and maximum relative acceleration in Tables 3-4.

The C.O.V.s of maximum relative displacement f or artificial earthquake ground accelerations of No.1, No3 and No.4 are shown in Figs. 11-13, respectively. From these figures, it is also clear that the C.O.V. of maximum relative displacement almost increases as the relative input intensity increases, namely the yield force F_y of restoring force is small. Furthermore, the C.O.V. of the maximum relative displacement changes sensitively to the period of linear system and it is generally seen that the

tendency for the C.O.V. becomes large for the short period range of structure. That is, in the short period case, if relative input intensity α increases, displacement will become large, but in the long period case, even if the relative input intensity changes, the maximum relative displacement does not change. From the C. O. V.s in the Tables 2-4, the C.O.V. of relative maximum displacement is the largest and the tendency which becomes small is seen with maximum relative velocity and acceleration.

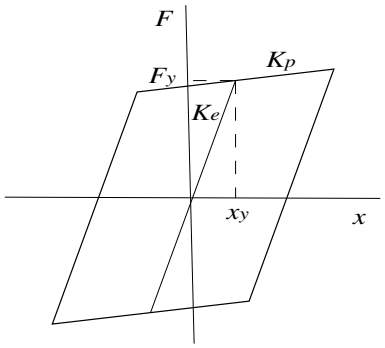

Figure9. Bi-linear model of elasto-plastic structure

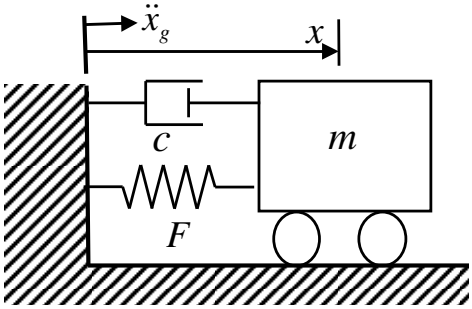

Figure10. SDOF model of bi-linear restoring force

Table 2. Coefficient of variation for maximum displacement

Period (s)	Relative input intensity	Type of generated ground motions				
		No.1	No.2	No.3	No.4	No.5
0.2	1.0	0.231	0.302	0.350	0.290	0.264
	1.2	0.223	0.332	0.3530	0.346	0.333
	1.5	0.268	0.324	0.314	0.379	0.393
	2.0	0.319	0.367	0.253	0.375	0.340
0.5	1.0	0.158	0.179	0.236	0.148	0.195
	1.2	0.180	0.195	0.288	0.169	0.192
	1.5	0.242	0.232	0.280	0.218	0.277
	2.0	0.283	0.257	0.310	0.232	0.294
1.0	1.0	0.179	0.177	0.154	0.139	0.100
	1.2	0.180	0.185	0.157	0.110	0.105
	1.5	0.182	0.209	0.203	0.110	0.122
	2.0	0.209	0.224	0.266	0.129	0.178

Table 3. Coefficient of variation for maximum velocity

Period (s)	Relative input intensity	Type of synthesized ground motions				
		No.1	No.2	No.3	No.4	No.5
0.2	1.0	0.046	0.042	0.061	0.094	0.093
	1.2	0.051	0.048	0.074	0.120	0.097
	1.5	0.053	0.055	0.095	0.169	0.107
	2.0	0.101	0.168	0.159	0.200	0.125
0.5	1.0	0.064	0.071	0.075	0.077	0.071
	1.2	0.074	0.071	0.071	0.100	0.068
	1.5	0.076	0.082	0.074	0.109	0.069
	2.0	0.110	0.104	0.099	0.126	0.083
1.0	1.0	0.121	0.108	0.079	0.065	0.093
	1.2	0.101	0.091	0.079	0.041	0.085
	1.5	0.066	0.084	0.076	0.079	0.077
	2.0	0.101	0.106	0.098	0.129	0.080

Table 4. Coefficient of variation for maximum absolute acceleration

Period (s)	Relative input intensity	Type of synthesized ground motions				
		No.1	No.2	No.3	No.4	No.5
0.2	1.0	0.008	0.007	0.0135	0.009	0.0085
	1.2	0.006	0.010	0.0199	0.012	0.0081
	1.5	0.011	0.017	0.0255	0.022	0.0136
	2.0	0.019	0.034	0.0327	0.035	0.0224
0.5	1.0	0.007	0.006	0.0068	0.007	0.0057
	1.2	0.007	0.007	0.0083	0.009	0.0063
	1.5	0.008	0.009	0.0103	0.011	0.0078
	2.0	0.013	0.013	0.0168	0.015	0.0104
1.0	1.0	0.166	0.131	0.0432	0.137	0.0946
	1.2	0.110	0.075	0.0081	0.078	0.0441
	1.5	0.042	0.022	0.0071	0.012	0.0071
	2.0	0.009	0.010	0.0085	0.010	0.0068

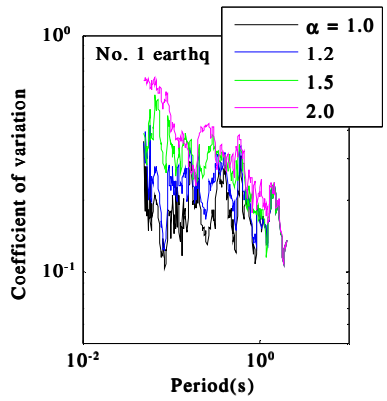

Figure11. C.O.V. of maximum displacements by No.1 artificial earthquake ground motions

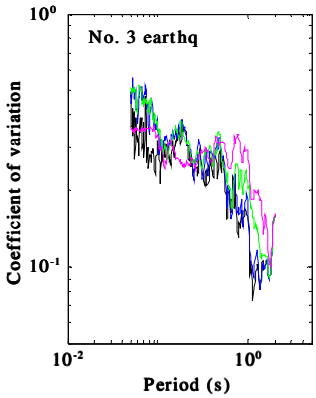

Figure12. C.O.V. of maximum displacements by No.3 artificial earthquake ground motions

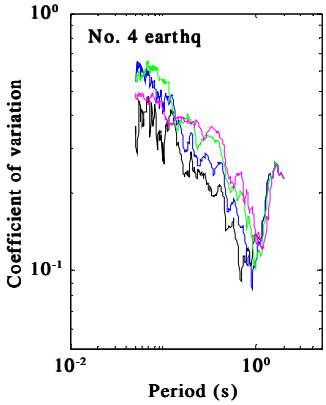

Figure13. C.O.V. of maximum displacements by No.4 artificial earthquake ground motions

The distributions of occurrence times of the maximum relative displacement of a system with natural period T_0=0.5 s to the artificial ground motions using the time-frequency characteristic of No. 1, No. 3, and No. 4 are shown in Figs. 14-16, the waveforms of displacement responses around these occurrence times are shown in Figs.17-19. Furthermore, the examples of their trajectories of mass on phase plane(x-x) are shown in Figs.20-22. From these figures, it is clear that the occurrence times of maximum displacement of the artificial earthquake ground accelerations generated by same time-frequency characteristic tend to become almost the same, and the displacement response shows as sine wave vibration of the own natural period decided by initial stiffness, and the tendency for the its maximum value to occur near immediately after the drift of the central point of sine wave vibration is seen. In these figures, red circles denote the point of yield of structure.

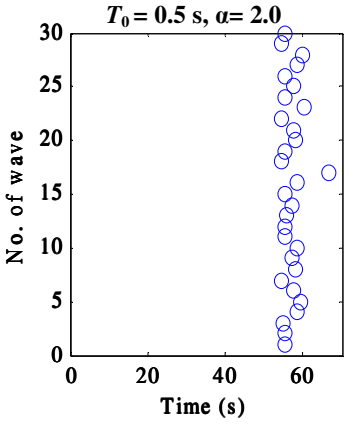

Figure14. Occurrence time of maximum displacement by No.1 artificial ground motions

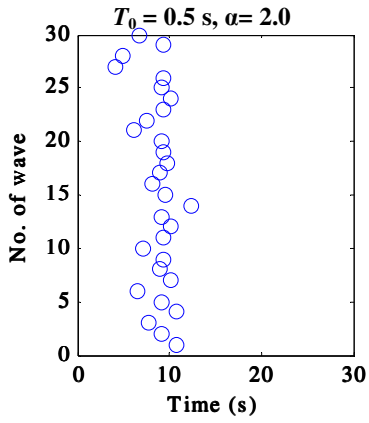

Figure15. Occurrence time of maximum displacement by No.3 artificial ground motions

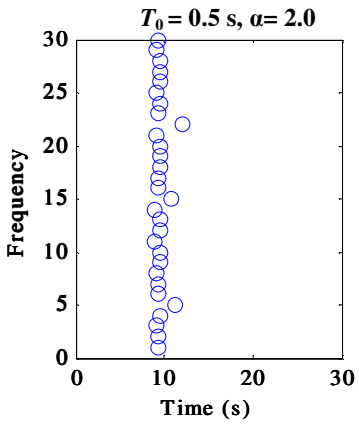

Figure16. Occurrence time of maximum displacement by No.4 artificial ground motions

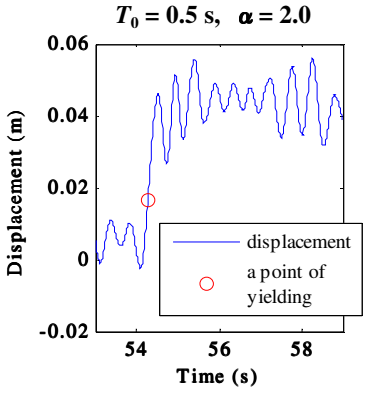

Figure17. Displacement around maximum displacement by No.1 artificial ground motions

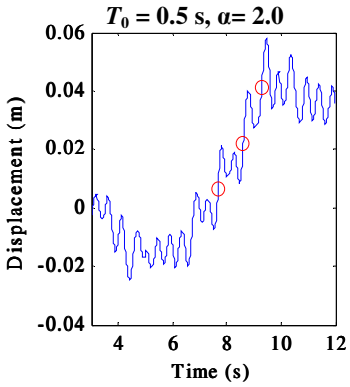

Figure18. Occurrence time of maximum displacement by No.3 artificial ground motions

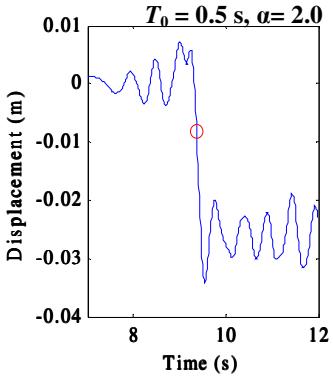

Figure19. Occurrence time of maximum displacement by No.4 artificial ground motions

Standard deviations and maximum values of the displacement responses and of the system with natural period of T_0=0.5 s to the artificial ground accelerations using the time-frequency characteristics of No. 1, No.3 and No. 4 seismic motions are shown in Figs. 23,-25, respectively. From these figures, it is clear that when the standard deviations of displacement responses are large like the step function at the time of drift by plastic displacement, and at this time the tendency

which the maximum responses occur is seen. Moreover, the time change of standard deviations of displacement response agrees with that of the maximum response.

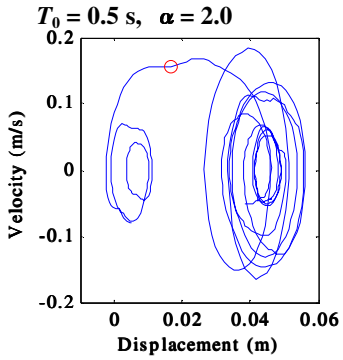

Figure20. Trajectory of mass on phase by No.1 artificial ground motions

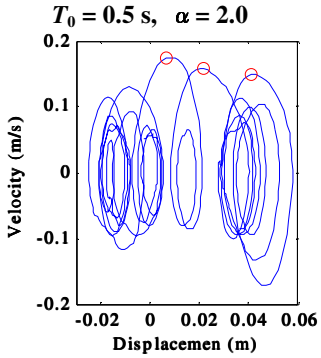

Figure21. Trajectory of mass on phase by No.3 artificial ground motions

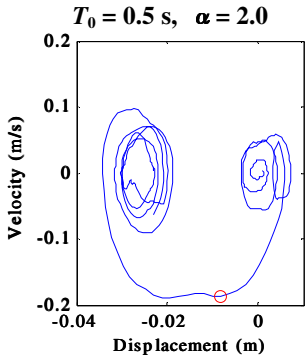

Figure22. Trajectory of mass on phase by No.4 artificial ground motions

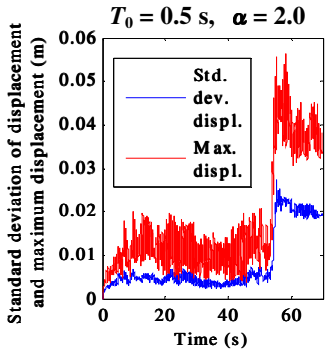

Figure23. Standard deviation of displacement by No.1 artificial ground motions

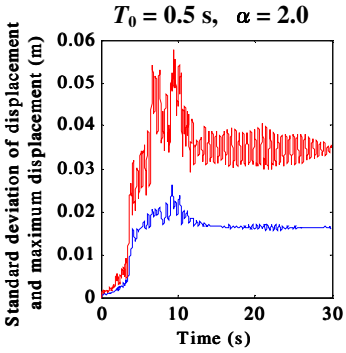

Figure24. Standard deviation of displacement by No.3 artificial ground motions

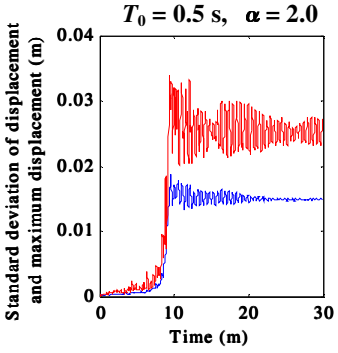

Figure25. Standard deviation of displacement by No.4 artificial ground motions

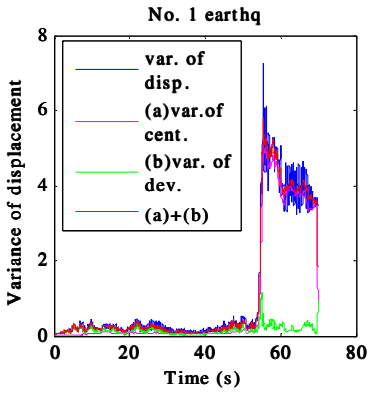

Figure26. Variance of decomposed displacement by No.1 artificial earthquake ground motions

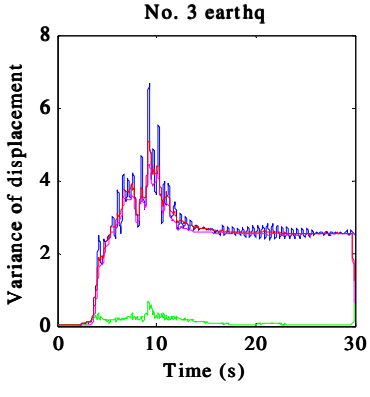

Figure27. Variance of decomposed displacement by No.3 artificial earthquake ground motions

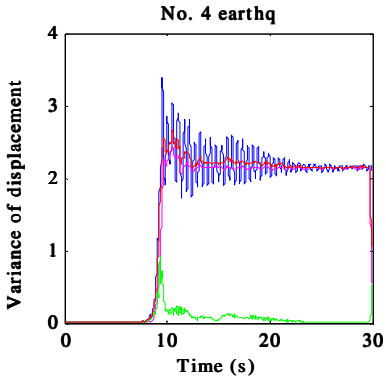

Figure28. Variance of decomposed displacement by No.4 artificial earthquake ground motions

Next, the displacement response is divided displacement into the average displacement during the time width of the periodic length of an own natural period and the its changed part around average displacement and these variance and these sum are compared with the variance of displacement response shown in Figs.26-28.

Variance of the displacement responses denoted by blue dotted curve shown in Figs. 26-28, variance of the average displacements (a), variance of its changed part (b) and these sum [(a)+(b)] are shown in Figs. 26-28, respectively.

In all cases of the artificial ground accelerations, the sum of variance of average displacement and variance of changed part around average displacement becomes smaller than the variation of the original displacement. This is considered that the average displacement and the changed part around it are not independent.

4. CONCLUSIONS

In this study, we choose five earthquake ground accelerations from the latest earthquakes whose maximum accelerations were large or which did serious damages to the structures. Using the time-frequency characteristics of these earthquake ground accelerations and Osaki's velocity response spectrum, five types of artificial earthquake ground acceleration are generated by our method and the coefficient of variation (C. O. V.) of maximum displacement, maximum velocity and maximum acceleration in elasto-plastic SDOF systems excited by these artificial ground motions are numerically evaluated. The main results are summarized as follows:
(1)The tendency of the C.O.V. of maximum displacement becomes large as the relative input intensity increases and the natural period of linear system decreases, is shown.
(2) It is clear that the occurrence times of maximum displacement of the artificial earthquake ground accelerations generated by same time-frequency characteristic tend to become almost the same. Also, the displacement response shows as sine wave vibration of the natural period decided by initial stiffness, and the tendency for the its maximum value to occur near immediately after the drift of the central point of sine wave vibration is seen.
(3) It is clear that when the variances of displacement responses are large as the step function at the time of drift by plastic displacement, and at this time the tendency which the maximum responses occur is seen. Moreover, the time change of variance of displacement response agrees with that of the maximum response.

In future, we will investigate the quantitative evaluation of these above results and will some suggestions for the maximum responses of the bi-linear system. Finally, in this study, we used the strong motion records by K-NET of National Research Institute for Earth Science and Disaster Prevention (NIED). Authors are grateful for NIED.

REFERENCES

Ichihashi, I., et al.(2010a). Response of elasto-plastic system excited by synthesized ground motion with given non-stationary time-frequency characteristics, *Journal of Applied Mechanics JSCE* **13**, 567-576.

Ichihashi, I., et al.(2010b). A study of Elasto-plastic Response of Single Degree of Freedom System Using Artificial Ground Motions with Given Time-frequency Characteristics. *ASME 2010 Pressure Vessels and Piping Division/ K-PVP Conference*, **PVP2010-25381**: 1-7.

Kimura, M. (1986). On control of the characteristics of the wave ingenerating simulated earthquake ground motions. *Journal of Structure and Construction Engineering of AIJ* **367,** 30-35.

Kitahara, T. and Itoh, Y. (2001). Study on variance of elasto-plastic response to a group of artificial earthquake ground motion compatible with same design response spectrum. *The Japan Concrete Institute* **23:3:**1237-1242.

Kubo, T, Hasegawa, H. and Yamamoto, M. (1989). Significance of Frequency Non-stationarity in Strong Earthquake Motions on the Inelastic Responses of a Structure : Part 2 : Inelastic Response of a Structure Subjected to the Synthetic Motions, *Annual Meeting of Architectural Institute of Japan*, **Structures I:**777-778.

Kuwamura, H., Takeda, T. and Sato, Y. (1997). Energy input rate in earthquake destructiveness-comparison between epicentral and oceanic earthquakes. *Journal of Structure and Construction Engineering of AIJ* **491**, 29-36.

Maeda, T., Sasaki, F. and Yamamoto, Y. (2002). Artificial ground motion with non-stationarity generated by the sinc wavelet." *Journal of Structure and Construction Engineering of AIJ*, **553**, 33-40.

Masuda, A. and Sone, A. (2002a). Wavelet-based Synthesis of Artificial Earthquake Motions Consistent with Response Spectra and Non-stationarity of Real Earthquake Records. *11th Japan Earthquake Engineering Symposium*, 527-532.

Masuda, A. and Sone, A. (2002b). Generation of Spectrum-compatible Earthquake Motion Using Wavelet Transform. *ASME Pressure Vessels and Piping Conference, Seismic Engineering-2002,* **PVP-445-1**: 175-180.

Ohsaki, Y. (1994). New introduction to spectrum analysis of earthquake ground motion. Kajimashupan. Japan